Generation and Detection of the Peroxyacetyl Radical in the Pyrolysis of Peroxyacetyl Nitrate in a Supersonic Expansion

Y. J. Hu, H. B. Fu, and E. R. Bernstein*

Department of Chemistry, Colorado State University, Colorado

Received: June 22, 2005; In Final Form: January 4, 2006

The peroxyacetyl radical (PA, $CH_3C(O)OO$) is generated by flash pyrolysis of peroxyacetyl nitrate (PAN, $CH_3C(O)OONO_2$) in a supersonic jet. The 0_0^0 $\tilde{A}^2A' \leftarrow \tilde{X}^2A''$ electronic transition for PA, at ca. 5582 cm^{-1}, is detected in a supersonically cooled sample by time-of-flight mass spectroscopy in the CH_3CO mass channel. Rotational envelope simulation results find that the rotational temperature for PA in its ground electronic and vibrational state is ca. 55 K. At ca. 330 °C, the thermal decomposition of PAN by flash pyrolysis in a heated nozzle with supersonic expansion is mainly by formation of PA and NO_2. The maximum yield of PA is obtained at this temperature. At higher temperatures (300−550 °C), an intense signal in the CH_2CO^+ mass channel is observed, generated by the decomposition of PA.

I. Introduction

The peroxyacetyl radical (PA, $CH_3C(O)OO^{\bullet}$), is one of the most abundant and important organic peroxy radicals in the atmosphere. PA can be generated by thermal decomposition of peroxyacetyl nitrate (PAN, $CH_3C(O)OONO_2$), another important atmospheric and combustion species.[1] Early combined matrix and thermodynamic studies of PAN suggest that its primary dissociation pathway is breaking the weakest O−N bond producing PA. Other possible (minor) decomposition channels involve the breaking of the O−O peroxy bond or formation of a six-membered-ring reactive intermediate (e.g., H3CC(O)OONOO).[2−4] Recently, von Ahsen et al.[5] have investigated PAN decomposition processes in detail by low-pressure flash thermolysis/matrix isolation techniques and density functional theory calculations. This study partly confirms the above conclusions.

PA has been characterized and studied for the most part by its UV absorption for the $\tilde{B}^2A'' \leftarrow \tilde{X}^2A''$ transition.[6] The UV transition of PA is broad and structureless, because the $\tilde{B}$ state is dissociative and little is learned about the structural and energetic properties of PA from these mostly dissociative kinetics studies. The $\tilde{A}^2A' \leftarrow \tilde{X}^2A''$ transition in the near-infrared does display resolved rotational and vibrational structure and can yield information on the nature of the PA radical. The $\tilde{A}^2A' \leftarrow \tilde{X}^2A''$ transitions of several peroxy radicals have been explored by both Hunziker[7] and Zalyubovsky et al.[8] The latter authors have employed cavity ring down spectroscopy to study the $\tilde{A}^2A' \leftarrow \tilde{X}^2A''$ transition of the PA radical at ca. 300 K: vibronic features and rotational envelope resolution are achieved in this experiment.[8] This near-infrared transition has a small transition cross-section ($\sigma \approx 10^{-21}$ to $10^{-20} cm^2$), but supersonic expansion UV/IR and VUV/vis two-photon ionization techniques, recently employed in our laboratory for the study of radicals[9] and metal oxide species,[10] have proven sensitive enough to detect species that are weakly absorbing in the infrared.

In this report, we present the origin spectrum for the $\tilde{A}^2A' \leftarrow \tilde{X}^2A''$ transition of the PA radical, accessed in a supersonic molecular beam and detected through multiphoton (VUV/IR) ionization fragmentation time-of-flight mass spectroscopy (TOFMS). We discuss this approach to PA detection and present a spectrum of PA cooled in the supersonic expansion. The thermal decompositions of PAN and PA in this flow system are also discussed.

II. Experimental Procedures

A. Precursor—Peroxyacetyl Nitrate (PAN) Preparation. PAN is prepared by the acid-catalyzed nitration of peracetic acid ($CH_3C(O)OOH$) in tridecane ($C_{13}H_{28}$) solvent. Synthesis of PAN is performed according to the method of Nielsen et al.[11] and Gaffney et al.,[12] slightly modified by Williams et al.[13] The yield is about 40%. Briefly, 3 mL of peracetic acid (32 wt % solution, Aldrich) is mixed with 20 mL of tridecane in a 250 mL round-bottom flask. The mixture is maintained at a temperature of 0 °C with an ice salt bath. Two milliliters of sulfuric acid (99.999%, Aldrich) is added to the flask, and then, 1.5 mL of nitric acid (90%, Aldrich) is slowly dripped into the flask over a period of 5 min. Nitrogen gas is slowly bubbled through the mixture during the reaction. Recently, we are generating the peracetic acid from acetic anhydride and hydrogen peroxide, as the latter chemicals are less expensive and they are much more stable than peracetic acid. After completion of the nitration reaction, the mixture is transferred to a 250 mL separatory funnel. The acid layer is separated from the tridecane layer, and the tridecane is washed 2 to 3 times with ∼25 mL of cold deionized water to remove traces of inorganic acids. The FT-IR spectrum of the solution displays strong absorption bands characteristic of PAN at 1830 and 1727 cm^{-1} and no absorption bands in the OH stretching region.[12]

The tridecane mixture containing PAN is dried with anhydrous magnesium sulfate and then filtered. This dry solution is stored in a refrigerator maintained at −20 °C. The solution can be employed as a direct source of gaseous PAN. PAN gas is transferred to a pulsed valve for supersonic expansion/photolysis or pyrolysis by bubbling the expansion gas (He or Ar) through the liquid sample maintained at 0 °C in an ice bath. Pure PAN can also be collected by bubbling He through the tridecane/PAN solution held at 0 °C and condensing PAN in a liquid nitrogen cooled trap.

10.1021/jp058196i CCC: $33.50
Published on Web 02/04/2006

B. Flash Pyrolysis Nozzle. The method of radical generation in a supersonic expansion employing flash pyrolysis was first demonstrated by Chen et al.[14] We have modeled our system for the synthesis of PA from PAN after their basic design. Briefly, a 2.5-cm-long alumina tube (Versus McDonald Co.) with a 4.5 mm o.d. and a 0.8 mm i.d is attached to a General Valve Series 9 solenoid valve. The attached tube and the valve are coaxial. Heater wire is wound around the Al_2O_3 extension tube and coated with alumina cement (Cotronics Co.). This setup can generate a temperature as high as ca. 800 °C inside the Al_2O_3 tube. The electrical resistance of the heater wire is independent of temperature, and temperatures below 1000 °C at the nozzle can be easily controlled. The heater assembly is in series with a ballast resistance (to prevent thermal runaway) and its temperature controlled by a Variac. The Al_2O_3 tube/wire assembly is preferable to a SiC tube directly heated within the 100−500 °C temperature range, because its temperature control is better in this range and Al_2O_3 is more chemically inert. Flow tube temperatures are measured by two thermocouples (Omega Co., type K), one of which is attached to the outside surface of the ceramic tube, and the other of which is placed inside the nozzle flow tube under the same conditions as those of the experiment. Both measured temperatures are the same within experimental error. The thermocouple (type K) employed has a temperature accuracy of ±2.2 °C or ±0.75%. During the experiment, the thermocouple inside of the nozzle flow tube is removed.

C. Generation of Peroxyacetyl ($CH_3C(O)OO$) Radicals. Both pyrolysis and photolysis can be used to generate many radicals from closed-shell precursors. These two techniques are often interchangeable. We have employed both of these approaches for the generation of methoxy, benzyl, methyl, cyclopentadienyl, NCO, and other radicals.[15]

Numerous experimental studies[5,16] have shown that thermal decomposition of PAN occurs only via an NO_2-producing reaction channel (O−N bond cleavage)

$$CH_3C(O)O_2NO_2(PAN) \rightarrow CH_3C(O)O_2^{\bullet}(PA) + NO_2 \qquad (1)$$

with no contribution from an NO_3-producing channel (O−O bond cleavage)

$$CH_3C(O)OONO_2 \rightarrow CH_3COO^{\bullet} + NO_3 \qquad (2)$$

even though the two channels are predicted to be nearly isoenergetic. All of our experimental results are consistent with this observation, but in fact, the ionization energies for NO_3 and CH_3CO_2 are not available. A 118 nm photon (10.5 eV) should be sufficient to ionize both of these species on the basis of the ionization energies of other similar ions. One can argue that thermal decomposition path (1) is favored over path (2), because path (1) proceeds without an activation barrier.[5] Additionally, the 248 nm photodissociation of PAN[17] demonstrates significant quantum yield for both channels ($\Phi(1) \approx 0.8$ and $\Phi(2) \approx 0.25$), and thus, pyrolysis seems to be the preferable method for the generation of PA from PAN.

D. Nonresonant Ionization Detection (NID- IR/NIR) Technique and Its Application for the Detection of PA Radicals. As pointed out above, the first excited electronic states of PA and other ROO• species generate $\tilde{A}^2A' \leftarrow \tilde{X}^2A''$ transitions that fall in the 1−2 μm (IR/NIR) spectral region. Tunable radiation in this wavelength range is conveniently generated with an optical parametric oscillator (OPO) pumped by a Nd:YAG laser at 532 nm (generated by doubling the fundamental output (1064 nm) of a Nd:YAG laser). Our laser system for this region of the spectrum consists of a seeded Quanta Ray Nd:YAG laser, a KDP doubler, and a Laser Vision OPO. This laser/nonlinear optical system converts the 1.064 μm radiation of the Nd:YAG fundamental output to tunable 0.71 to 2.10 μm radiation. The OPO consists of two interchangeable sets of nonlinear crystals ($KTiOPO_4$). All OPO crystals and tuning mirrors are computer-controlled. The nominal bandwidth of this laser output is 3 cm^{-1} for both signal and idler beams. Using an injection seeded Nd:YAG pump source reduces the output bandwidth to 2 cm^{-1}, and a grating tuning mirror assembly in place of the rear OPO optic reduces the output bandwidth further to 0.4 cm^{-1}. The output energy of this laser system is ∼4 mJ/pulse from 1.0 to 2.1 μm, and the laser pulse duration is ca. 10 ns.

This OPO laser system provides a widely tunable, pulsed, high peak power, IR/NIR source that can be employed to generate significant population for excited ground electronic state vibrational levels and low-lying excited electronic states (e.g., the $\tilde{A}$ state of ROO•). Nonresonant ionization detected infrared and near-infrared (NID-IR/NIR) spectroscopy has been employed to study ground-state vibrational energy levels (overtones and combinations) of molecules in the 1−2 μm spectral range.[18] In the present study, we employ a technique similar to NID-IR/NIR for detecting PA radicals through the $\tilde{A} \leftarrow \tilde{X}$ absorption. The ionization energy of PA is about 11 eV,[19] and thus, we employ 118 nm (10.5 eV) photons, the ninth harmonic of the 1.064 nm Nd:YAG fundamental, to serve as the single-photon nonresonant ionization source, and use the OPO to generate 0.7 eV photons for the $\tilde{A}^2A' \leftarrow \tilde{X}^2A''$ transition of PA for ion generation and detection. Generation of 118 nm light has been described previously;[20] pulse energy is estimated at ca. 1 μJ (10^{12} photon/pulse). The VUV laser is fixed in wavelength, and the IR OPO is scanned. The ion signal increases significantly as the $\tilde{A}^2A' \leftarrow \tilde{X}^2A''$ PA resonance is obtained.

Ions created by the above multiphoton process are extracted from the ionization region of the time-of-flight mass spectrometer (TOFMS) at 4 keV total energy. Mass-resolved detection is achieved by using a Galieo Electro-Optics microchannel plate (MCP) at the end of a 1.5 m flight tube. In our experiment, the pulsed nozzle and lasers are operated at 10 Hz and synchronized using a digital delay generator (SRS DG535, Stanford Research System). The data acquisition scheme for infrared spectroscopy is similar to that used to record REMPI (resonance enhanced multiphoton ionization) spectroscopy described in detail from this laboratory.[15]

III. Results and Discussion

Data for the detection and identification of PA have been collected by ionization at ca. 300 nm (UV) and at 118 nm (VUV). Both wavelengths are useful for this process because ionization occurs via different pathways in each instance, and thus additionally confirms the presence of PA in the beam due to PAN pyrolysis. As indicated below, the PA^+ ion is not stable and the $\tilde{B}$ state of PA is dissociative, so PA is not directly detected in these experiments except through its $\tilde{A} \leftarrow \tilde{X}$ transition in the near-IR.

A. Mass Spectra of PAN and PA. PA has a repulsive state ($\tilde{B}$ state) in the UV region, and its fragment, CH_3CO, can be detected via resonance enhanced multiphoton ionization (REMPI) employing UV radiation.[21] Figure 1a presents the mass peak intensities of species related to the pyrolysis of PAN in a heated supersonic jet at different temperatures as detected by TOFMS. Species are multiphoton fragmented and ionized by ∼300 nm focused UV light (∼2 mJ/pulse) generated from a doubled dye

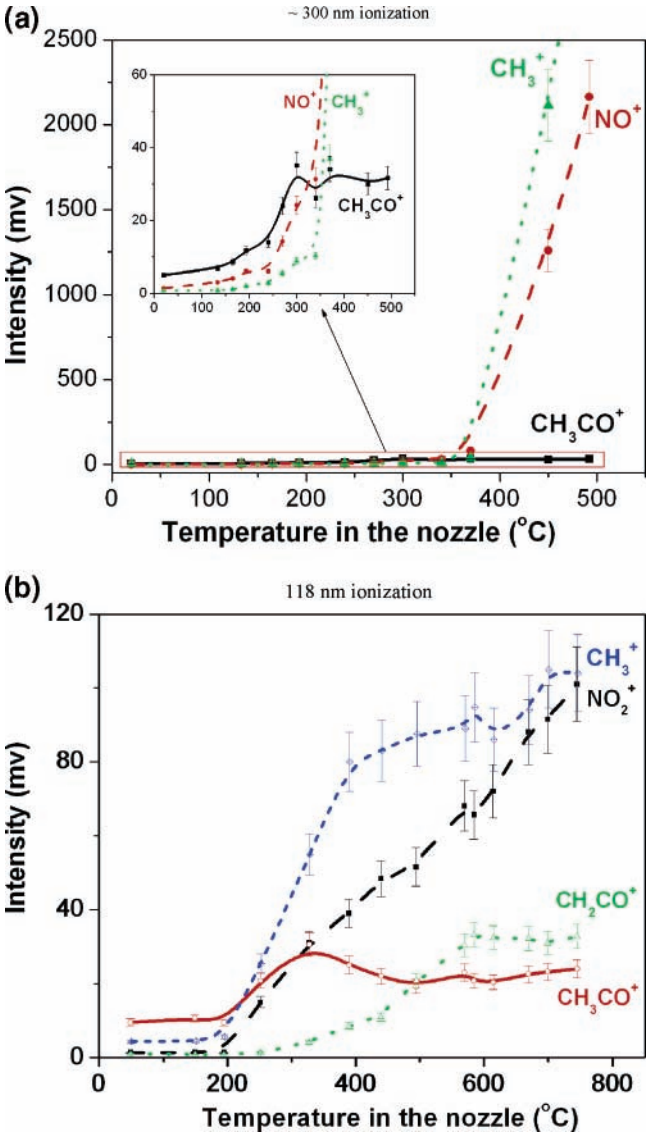

Figure 1. TOFMS signal intensities of species detected following thermal decomposition of PAN with different temperatures in the nozzle. The species are photoionized by (a) UV radiation, 332.75 nm for CH_3CO, 333.25 nm for NO, 333.5 nm for CH_3, respectively; (b) VUV radiation. The measured error is ±5%.

laser output. The wavelengths employed to detect the various ions are as follows: 333.25 nm for NO^+;[23] 332.75 nm for CH_3CO^+;[21] and 333.5 nm for CH_3^+.[22] The fragments NO, CH_3CO, and CH_3 have strong (single and mulitphoton) absorptions in this spectral range. As temperature in the nozzle is increased from 150 to 300 °C, CH_3CO^+ and NO^+ grow in concentration in a parallel fashion, while the increase in CH_3^+ intensity is slower than that of CH_3CO^+ and NO^+. At temperatures above 300 °C, CH_3CO^+ intensity becomes approximately constant as CH_3^+ and NO^+ intensity increase significantly in a parallel fashion. These overall results can be interpreted by the following considerations. For temperatures below ~300 °C inside the nozzle extension heater tube, PAN is thermally dissociated to PA and NO_2. The PA radical is unstable under UV radiation, and it photodissociates to CH_3CO and O_2 before being ionized; therefore, only CH_3CO ions can be observed. Ionization of NO_2 with 10 ns UV light pulses generates only NO^+. Both CH_3CO^+ and NO^+ peak widths in the mass spectra are ~23 ns, while the peak width of CH_3^+ is ~10 ns (shown in Figure 2). Both CH_3CO and NO have extra translational energy due to photodissociation, while CH_3 is cooled by the nozzle expansion.

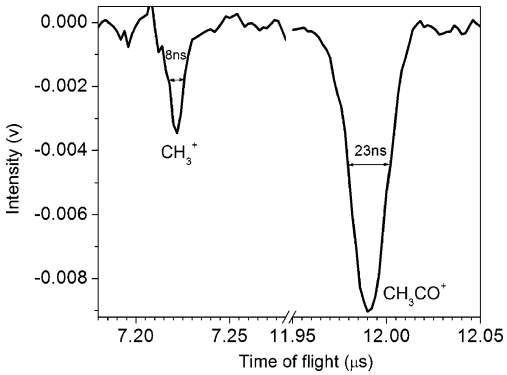

Figure 2. Mass spectrum of PAN decomposition products by flash pyrolysis in the heated nozzle. The temperature inside the extension tubing of the nozzle is 390 °C; UV radiation at 333.75 nm, is resonance for CH_3CO radicals.

These features in the TOF mass spectra strongly support the analysis above. With temperatures above 300 °C, the fate of the PA radical is different: PA radicals are thermally dissociated in the nozzle to yield CH_3, CO, and O_2 species. Thus, an intense signal for CH_3^+ is recorded in the mass spectrum as the temperature in the nozzle is increased above 300 °C. At 300 °C, the resident time of species in the flow tube is estimated as less than 20 μs,[24] and the maximum yield of PA is obtained.

Given the above laser excitation and ionization conditions, ~330 nm, and the thermal decomposition behavior of PAN and PA, the three species detected as PA and PAN fragments are generated by different multiphoton ionization processes. CH_3 is detected by a (2 + 1) multiphoton ionization: CH_3 is generated mostly in the nozzle by thermal decomposition of PA at $T > 300$ °C. CH_3CO and NO are generated by photolysis of PA and in the NO_2 ionization process, respectively, requiring one photon for photolysis and three photons for ionization. Additionally, the cross-sections for these processes are different for each species, and thus, the extrapolation from TOFMS signal intensities to concentration is difficult to make. Nonetheless, the ~330 nm generated TOF mass spectra confirm the presence of PA in the expansion.

The same species can be detected employing 118 nm single-photon ionization (and possible fragmentation). Since the ionization energies of these species are all below 10 eV and the 118 nm light is of low fluence (ca. 10^{12} photons/pulse), single-photon nonresonant ionization of CH_3, NO_2, CH_3CO, and PA can be anticipated. Additionally, the cross-sections for ionization of these species under VUV radiation can be estimated to be similar. Pyrolysis of PAN in the heated flow system can thus be monitored by 118 nm single-photon ionization and mass analysis of the ensuing ions. Figure 3 shows mass spectra of the thermal decomposition products of PAN in a flash pyrolysis tube generated by single-photon fragmentation and ionization with 118 nm light. Figure 1b presents a plot of the intensities of species produced by thermal decomposition of PAN at different temperatures, detected with 118 nm light and TOFMS. For a 250 °C pyrolysis, the ions CH_3CO^+, CH_3^+, and NO_2^+ are observed. As the temperature is increased to 500 °C, a feature at mass channel CH_2CO^+ appears (see Figure 3). This observation suggests that PA can also be dissociated to CH_2CO and HO_2 at temperatures higher than ~300 °C and the species CH_2CO (ketene, perhaps) can be ionized by 118 nm light.[26] Note that the CH_2CO^+ peak in Figure 3 grows as temperature is increased. Unfortunately, the ionization energy for $HO_2^\bullet$ is 11.35 eV,[19] and we cannot observe this signal with single-photon 10.5 eV ionization energy. CH_2CO is not observed

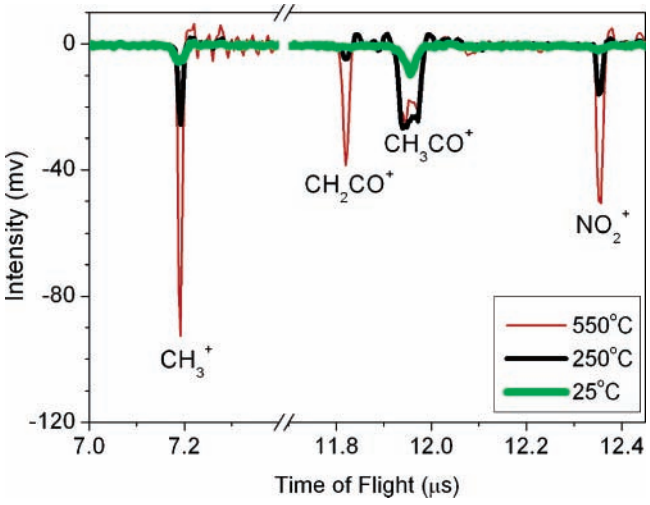

Figure 3. TOFMS of PAN decomposition products with different temperatures inside the nozzle extension tube. The species are ionized by 118 nm radiation.

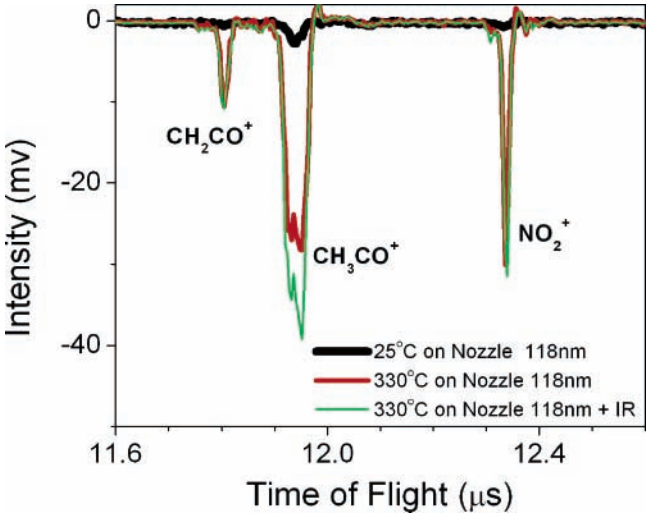

Figure 4. TOFMS of PAN and PA radical decomposition products photoionized (1 + 1) by 118 nm + near-IR light.

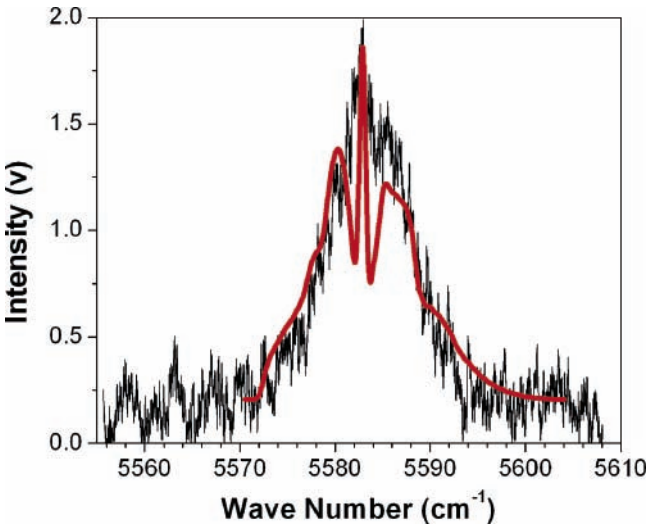

Figure 5. Spectrum of the origin of the $\tilde{A}^2A' \leftarrow \tilde{X}^2A''$electronic transition of peroxyacetyl and its simulated rotational contour. The simulation results show the rotational temperature of PA radicals generated in the nozzle is ca. 55 k. The spectrum is detected in the CH_3CO^+ mass channel.

under ~300 nm, as it is photodissociated by UV light.[26] From Figure 1b, at 300 °C intensities of peaks representing CH_3CO^+ are maximum. As temperature is increased beyond 300 °C, peak intensities representing CH_2CO^+ increase steeply with temperature. For temperatures above 600 °C, the intensity of CH_2CO^+ does not change. The intensity of the CH_3^+ mass peak increases steeply at temperatures below 400 °C but does not change between 400 and 600 °C. CH_3^+ intensity does increase steeply, however, at temperatures over 600 °C. Another product from this thermal decomposition of PAN is NO_2 (thermally stable at this temperature range), which can be ionized by 118 nm photons, and a 46 amu feature (NO_2^+) is observed in the mass spectrum given in Figure 3. NO_2 intensity increases with temperature over the temperature range explored.

All these results are consistent with the analysis reported in ref 8, which suggests that secondary reactions become important for PAN thermal dissociation under high-temperature conditions. At temperatures below 400 °C, PA radicals can thermally decompose to CH_3, CO, and O_2. At moderate temperatures (400 to 600 °C), the fate of PA can unfold along two pathways: (1) partial decomposition of PA to CH_3, CO, and O_2; and (2) partial decompsotion of PA to CH_2CO and HO_2. For temperatures higher than 600 °C, CH_2CO can also be thermally decomposed. Additionally, the CH_3 species could also be generated in a second decomposition channel for PAN: the radical CH_3CO_2 will be generated in this channel, and calculations predict that this unstable radical will subsequently generate CO_2 and CH_3.[5]

At low temperature (<300 °C), the main product of PAN thermal decomposition should be PA: the parent PA ion ($CH_3C(O)OO^+$) does not appear in the mass spectrum for ionization at 118 nm. Ab initio calculation shows that PA does not form a stable ion.[27] The broad feature (~40 ns) for CH_3CO^+ in the mass spectrum (Figure 3) can be explained as due to either extra kinetic energy for CH_3CO^+ as PA fragments or slow (~1 μs) fragmentation of the PA radical in the ion source region of the TOFMS. The increased width to this particular feature in Figure 3 supports the above suggested behavior for PAN and PA in the expansion. The doublet shape for the CH_3CO^+ mass spectral peak is indicative of excess kinetic energy, supporting the first explanation for its width.

B. Vibronic Spectrum of PA for the $\tilde{A}^2A' \leftarrow \tilde{X}^2A''$ Transition. Mass spectra of PAN and PA obtained with 118 nm and NIR irradiation simultaneously at the ion source region of the TOFMS are presented in Figure 4. With the nozzle at room temperature, the intensity of the ionized PAN decomposition products CH_2CO^+, CH_3CO^+, and NO_2^+ is quite low. These features arise from a background of PAN (ionization energy of 11.2 eV[28]). On the basis of the results above, the concentration of PA radicals in the molecular beam generated from flash pyrolysis of PAN is the maximum at ca. 330 °C. Thus, in this experiment, the temperatures are controlled at ca. 330 °C. With added IR radiation at 5578.2 cm $^{-1}$, the peak intensity of the CH_3CO^+ mass channel signal increases by 30%, although the mass channel signals for CH_2CO^+ and NO_2^+ remain constant. These data imply that CH_3CO comes from photodissociation of PA and the others do not. Figure 5 presents the 0_0^0 absorption feature of PA at ca. 5582 cm^{-1}, obtained by detecting the CH_3CO^+ mass channel signal and scanning the IR laser with 118 nm ionizing radiation simultaneously. The spectrum shows peak absorption at 5582.5 cm^{-1}, which corresponds to the 0_0^0 transition for the $\tilde{A}^2A' \leftarrow \tilde{X}^2A''$ transition of PA.[7,8] This result is consistent with that reported by ref 8. The line width of IR light is ca. 0.4 cm^{-1}, and the fwhm value of the 0_0^0 peak in the spectrum is ca. 7.3 cm^{-1}. Simulated rotational contours for this transition[29] show that the PA species has a ca. 55 K rotational

temperature. The values of rotational constants of the PA radicals used for simulation are adapted from ref 8.

Ab initio calculation suggests that the all-trans conformer of PA is the more stable, and the measured spectrum above is assigned to the trans conformer of PA. In the supersonic molecular beam, the equilibrium population of the cis conformer of PA is very small, and its transition has a lower energy than that of the trans conformer.[8] Unfortunately, our OPO system has very low power output in this spectral range. The vibrational temperature of PA in the expansion must be low, as well, since no hot bands are observed in this spectrum. A more detailed spectrum with vibronic assignments for this PA transition will be presented soon.[27]

IV. Conclusions

Peroxyacetyl radicals are generated by the flash pyrolysis of peroxyacetyl nitrate in a supersonic expansion. At nozzle temperatures ca. 330 °C, the maximum yield of PA in the pyrolysis flow system is obtained. The 0_0^0 $\tilde{A}^2A' \leftarrow \tilde{X}^2A''$ electronic transition for the PA radical at ca. 5582 cm^{-1} is detected in the supersonically cooled sample in the CH_3CO mass channel. The rotational temperature for PA in its ground electronic and vibrational state is ca. 55 K. The primary decomposition channel at low temperature ($\leq$300 °C) for PAN is the formation of the PA radical and NO_2. At higher temperatures (300−550 °C), an intense ketene (CH_2CO) feature can be observed, produced by the decomposition of PA.

Acknowledgment. This work is supported by grants from the U.S. NSF and the Philip Morris, U.S.A., Research Management Group. We thank Prof. G. B. Ellison and Drs. J. B. Burkholder and G. Tyndall at NOAA for helpful suggestions on the synthesis and manipulation of PAN.

References and Notes

(1) Heuss, J. M.; Glasson, W. A. *Environ. Sci. Technol.* **1968**, *2*, 1109. Taylor O. C. *J. Air Pollut. Control Assoc.* **1969**, *19*, 347.

(2) Grosjean, E.; Grosjean, D.; Fraser, M. P.; Cass, G. R. *Environ. Sci. Technol*. **1996**, *30*, 1731.

(3) Orlando, J. J.; Tyndall, G. S.; Galvert, J. G. *Atmos. Environ.* **1992**, *26A*, 3111.

(4) Roberts, J. M.; Bertman, S. B. *Int. J. Chem. Kinet.* **1992**, *24*, 297.

(5) von Ahsen, S.; Willner, H.; Francisco, J. S. *J. Chem. Phys.* **2004**, *21*, 2048.

(6) Lightfoot, P. D.; Cox, R. A.; Crowley, J. N.; Destriau, M.; Hayman, G. D.; Jenkin, M. E.; Moortgat, G. K.; Zabel, F. *Atmos. Environ.* **1992**, *26A*, 1805.

(7) Hunziker, H. E.; Wendt, H. R. *J. Chem. Phys.* **1976**, *64*, 3488.

(8) Zalyubovsky, S. J.; Glover, B. G.; Miller, T. A. *J. Phys. Chem. A* **2003**, *107*, 7704.

(9) Fu, H. B.; Hu, Y. J.; Bernstein, E. R. IR/UV Double resonance spectroscopy of the methyl radical: Determination of ν_3 in the $3p_z$ Rydberg state. *J. Chem. Phys.* **2005**, *123*, 234307.

(10) Matsuda, Y.; Bernstein, E. R. *J. Phys. Chem. A* **2005**, *109*(17), 3803.

(11) Nielsen, T.; Hansen, A. M.; Thomsen, E. L. *Atmos. Environ.* **1982**, *10*, 115.

(12) Gaffney, J. S.; Fajer, R.; Senum, G. I. *Atmos. Environ.* **1984**, *18*, 215.

(13) Williams, J.; Roberts, J. M.; Bertman, S. B. *J. Geophys. Res.* **2000**, *105*, 28943.

(14) Kohn, D. W.; Clauberg, H.; Chen, P. *Rev. Sci. Instrum.* **1992**, *63*, 4003.

(15) Shang, Q. Y.; Moreno, P. O.; Bernstein, E. R. *J. Am. Chem. Soc.* **1994**, *116*, 311. (b) Shang, Q. Y.; Bernstein, E. R. *J. Chem. Phys.* **1994**, *100*, 8625. (c) Disselkamp, R.; Bernstein, E. R.; Seeman, J. I.; Secor, H. V. *J. Chem. Phys.* **1992**, *97*, 8130.

(16) Tischer, G.; Nwankwoala, A. V. *Atmos. Environ.* **1995**, *29*, 3277. (b) Cox, R. A.; Roffey, M. J. *Environ. Sci. Technol.* **1977**, *11*, 1976. (c) Dellinger, B.; King, D. S.; Hochstrasser, R. M.; Smith, A. B. *J. Am. Chem. Soc*. **1977**, *99*, 3198.

(17) Mazely, T. L.; Friedl, R. R.; Sander, S. P. *J. Phys. Chem. A* **1997**, *101*, 7090.

(18) Tanabe, S.; Ebata, T.; Fujii, M.; Mikami, N. *Chem. Phys. Lett.* **1993**, *215*, 347.

(19) Litorja, M.; Ruscic, B. *J. Electron Spectrosc. Relat. Phenom.* **1998**, *97*, 131.

(20) Matsuda, Y.; Shin, D. N.; Bernstein, E. R. *J. Chem. Phys.* **2004**, *120*, 4165.

(21) Li, R. H.; Wu, J. C.; Chang, J. L.; Chen, Y. T. *Chem. Phys.* **2001**, *274*, 275.

(22) Chen, P.; Colson, S. D.; Chupka, W. A.; Berson, J. A. *J. Phys. Chem.* **1986**, *90*, 2319.

(23) Ledingham, K. W. D.; Kosmidis, C.; Georgiou, S.; Couris, S.; Singhal, R. P. *Chem. Phys. Lett.* **1995**, *247*, 555, and references therein.

(24) Rohrs, H. W.; Wickham-Jones, C. T.; Ellison, G. B. *Rev. Sci. Instrum.* **1995**, *66*, 2430.

(25) http://webbook.nist.gov/chemistry.

(26) Hayden, C. C.; Neumark, D. M.; Shobatake, K.; Sparks, R. K.; Lee, Y. T. *J. Chem. Phys.* **1982**, *76*, 3607.

(27) Hu, Y.; Fu, H.; Bernstein, E. R. Spectrum of the A−X vibronic transition of peroxyacetyl radicals in the near-IR range. *J. Chem. Phys*. To be published.

(28) Li, Y.; Li, H.; Sun, Q.; Wang, D. *Acta Chim. Sin.* **2003**, *61*, 1492.

(29) Stakhursky, V. L.; http://molspect.mps.ohio-state.edu/goes/specview.html.